Programmed population control by cell–cell communication and regulated killing

Lingchong You[1], **Robert Sidney Cox III**[2], **Ron Weiss**[3] & **Frances H. Arnold**[1]

[1]*Division of Chemistry and Chemical Engineering and* [2]*Division of Biology, California Institute of Technology, Pasadena, California 91125, USA*
[3]*Departments of Electrical Engineering and Molecular Biology, Princeton University, Princeton, New Jersey 08544, USA*

De novo engineering of gene circuits inside cells is extremely difficult[1–9], and efforts to realize predictable and robust performance must deal with noise in gene expression and variation in phenotypes between cells[10–12]. Here we demonstrate that by coupling gene expression to cell survival and death using cell–cell communication, we can programme the dynamics of a population despite variability in the behaviour of individual cells. Specifically, we have built and characterized a 'population control' circuit that autonomously regulates the density of an *Escherichia coli* population. The cell density is broadcasted and detected by elements from a bacterial quorum-sensing system[13,14], which in turn regulate the death rate. As predicted by a simple mathematical model, the circuit can set a stable steady state in terms of cell density and gene expression that is easily tunable by varying the stability of the cell–cell communication signal. This circuit incorporates a mechanism for programmed death in response to changes in the environment, and allows us to probe the design principles of its more complex natural counterparts.

Our circuit (Fig. 1a) programmes a bacterial population to maintain a cell density that is lower than the limits imposed by the environment (for example, by nutrient supply). The LuxI protein of the well-characterized LuxI/LuxR system from the marine bacterium *Vibrio fischeri*[13,14] synthesizes a small, diffusible acyl-homoserine lactone (AHL) signalling molecule. The AHL accumulates in the experimental medium and inside the cells as the cell density increases. At sufficiently high concentrations, it binds and activates the LuxR transcriptional regulator, which in turn induces the expression of a killer gene (*E*) under the control of a *luxI* promoter (p_{luxI})[15]. Sufficiently high levels of the killer protein cause cell death.

We implemented the circuit using a two-plasmid system (Fig. 1b), where pLuxRI2 expresses LuxI and LuxR upon induction by isopropyl-β-D-thiogalactopyranoside (IPTG), and p*lux*CcdB3 responds to activated LuxR (at sufficiently high cell density) and causes cell death. The *lacZα–ccdB* killer gene codes for a fusion protein of LacZα and CcdB. The LacZα portion of the fusion protein retains the ability to complement LacZΔM15 in appropriate cell strains (for example, Top10F′ cells), allowing the measurement of fusion protein levels using a LacZ assay (see Methods). The CcdB portion retains the toxicity of native CcdB, which kills susceptible cells by poisoning the DNA gyrase complex[16].

A simple mathematical model predicted that the system would reach a stable cell density for all realistic parameter values (see Methods), although it might go through damped oscillations while approaching the steady state. Experiments confirmed our predictions. Figure 2a shows the growth of Top10F′ cells containing the population-control circuit at pH 7.0. As anticipated, the uninduced culture (circuit OFF) grew exponentially and reached the stationary phase upon nutrient exhaustion. The induced culture (circuit ON) grew almost identically, until its density reached a threshold (at 7 h). It then deviated sharply from the OFF culture and briefly went through a damped oscillation (between 7 h and 24 h) of at least one

cycle before reaching a steady-state density about ten times lower than that of the OFF culture. The measured peak density (at 10 h) was twofold higher than the measured floor (12.5 h), a difference significantly greater than measurement variations. The steady state was maintained for more than 30 h: the variation in cell density between 28 h and 62 h was <5%, which was smaller than typical measurement variations of individual data points. The transient dynamics of circuit-ON growth was captured well in simulation, where the AHL degradation rate constant (d_A) was adjusted for the simulation to match the experiment in the steady-state circuit-ON cell density. Intracellular levels of LacZα–CcdB for the ON culture, measured in terms of LacZ activity, reached a steady state after an overshoot (Fig. 2b), again predicted by the simulation. The basal level of LacZα–CcdB expression in the OFF culture was negligible for all time points.

The growth curves and the LacZα–CcdB time courses illustrate the tight yet dynamic coupling between population dynamics and intracellular expression of the LacZα–CcdB killer protein. A level of the killer protein lower than steady state allows the population to grow; conversely, its excessive production decreases cell density. After some delay, the decline in cell density leads to a decrease in AHL concentration, which in turn leads to reduced levels of the killer protein, allowing the population to recover. Continuous production and degradation (or death) of each circuit component are essential for the observed homeostasis, and they are closely coupled. Any perturbation that decouples or overrides these processes will disrupt circuit function. For example, a circuit without *luxI* (thus lacking a communication link) could not control growth (data not shown). Also, we observed that 200 nM exogenous AHL, which was not toxic to cells without the circuit or with the circuit OFF, completely prevented growth with the circuit ON (data not shown). This is expected, because a high level of AHL would activate LuxR and lead to overproduction of the killer protein. This observation also confirms that the killer protein production rate was limited by AHL synthesis in circuit-ON growth, a key assumption in our mathematical model.

Circuit function could also be delicately manipulated in a predictable fashion. Our model predicted that the steady-state cell density would increase nearly proportionally with the AHL degradation rate constant (see Methods). Thus, AHL serves as an external 'dial' to operate the circuit: AHL degradation affects cell–cell communication, and rapid AHL breakdown can disrupt it
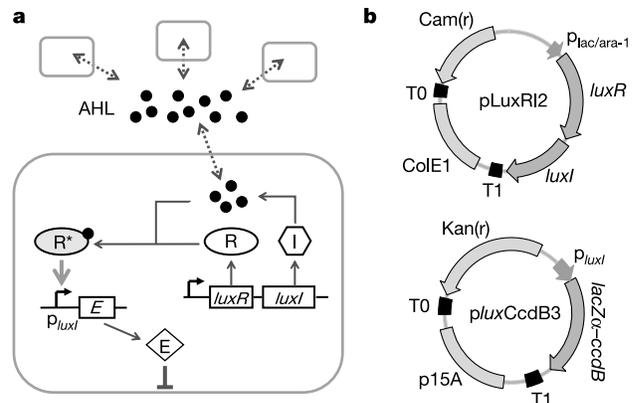

Figure 1 A population-control circuit programmes population dynamics by broadcasting, sensing and regulating the cell density using cell–cell communication and negative feedback. **a**, Schematic diagram of the circuit. *E* is a 'killer' gene. I, R and R* represent LuxI, LuxR and active LuxR, respectively. Filled circles represent AHL. **b**, Experimental implementation with two plasmids, pLuxRI2 and p*lux*CcdB3. *luxI* and *luxR* are under the control of a synthetic promoter $p_{lac/ara-1}$[32], and the killer gene (*lacZα–ccdB*) is under the control of p_{luxI}[15]. T0 and T1 are transcription terminators. See text for details.

 1

completely. Degradation of AHL is facilitated by hydrolytic enzymes[17,18] or by increasing the medium pH[19]. Confirming the model prediction, a moderate increase in the medium pH (6.2 to 7.8) significantly increased (~fourfold) steady-state cell densities of the ON cultures, but caused only minor changes in those of the OFF cultures (Fig. 3a–e, Table 1). For each pH value, circuit-ON populations reached a steady state after 28 h, and the variation in cell density afterwards was smaller than typical measurement variations. Similar to the pH 7.0 case, the ON cultures grew almost identically to the OFF cultures at low cell density, but deviated from the latter at high density. Again, simulations captured the experimental behaviour (Fig. 3a–d), with adjustment only of the AHL degradation rate constant (Table 1).

Our model predicted that, unlike cell density, intracellular levels of the killer protein would remain roughly constant as pH varied. At steady state, $E_s = k/d \, (1 - N_s/N_m) \approx k/d$, the ratio of the growth and killing rate constants (assuming that the circuit-ON cell density is far below the carrying capacity; that is, $N_s/N_m \ll 1$). Thus if pH did not significantly affect the growth or killing rate constants, the killer protein would reach a concentration of k/d, independently of pH. Experimental results showed that LacZα–CcdB for different pHs reached similar levels after about 28 h (Fig. 3f–i, Table 1). Nevertheless, the pH changes affected other measured parameters, including k, N_m and more notably N_s (Table 1). To account for the effects of these changes on killer protein expression, we normalized LacZ activity with respect to $k(1 - N_s/N_m)$. According to the model, the normalized LacZ activity should remain constant if pH does not affect the killing rate constant (because $E_s/(k(1 - N_s/N_m)) = 1/d$). Supporting the prediction, normalized LacZ activities were nearly identical for different pHs (Fig. 3j). Except for pH 8.05, these values were statistically indistinguishable ($P = 0.26$). The slightly, but significantly, higher ($P = 8.6 \times 10^{-4}$) normalized LacZ activity at pH 8.05 suggests that the killer protein was less toxic (smaller d).

Construction of *de novo* gene circuits can be used to decode 'design principles' of biological systems[20–22]. Studies have demonstrated the feasibility of building gene circuits that lead to stable[1], bistable[2–4] or oscillatory[3,5] gene expression, act as a digital logic inverter[6,7] or a metabolic controller[8], or provide better-regulated gene expression systems[9]. They have also revealed major hurdles to achieving reliable circuit behaviour, such as noise in cellular processes and cell-to-cell variation[10–12]. Here we addressed these iss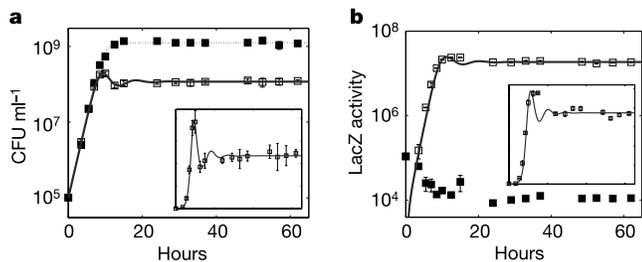ues by using cell–cell communication to coordinate behaviour across the population. By coupling gene expression with population dynamics, cell–cell communication integrates the entire population as an essential component of the population-control circuit. This coupling enables the circuit to function reliably at the population level by exploiting cell heterogeneity in terms of their size, age, plasmid copy number, gene expression and response to the killer protein. Such phenotypic variations, which interfere with the functioning of circuits lacking a communication mechanism, are actually required for the population-control circuit to work. The outcome of circuit function is binary for any given cell: it lives or dies (judged by the ability to form a colony). If all cells had the same phenotype, the circuit would fail to achieve a stable cell density because the population would become extinct once the killer protein concentration reached a critical threshold. And because of the coupling, the circuit can function only at the population level. This is supported by experimental data: under each set of conditions, growth of the circuit-ON culture only deviated from that of the OFF culture when cell density was sufficiently high (Figs 2 and 3). If the circuit had functioned inside each cell autonomously, growth of the two cultures would have deviated from the beginning.
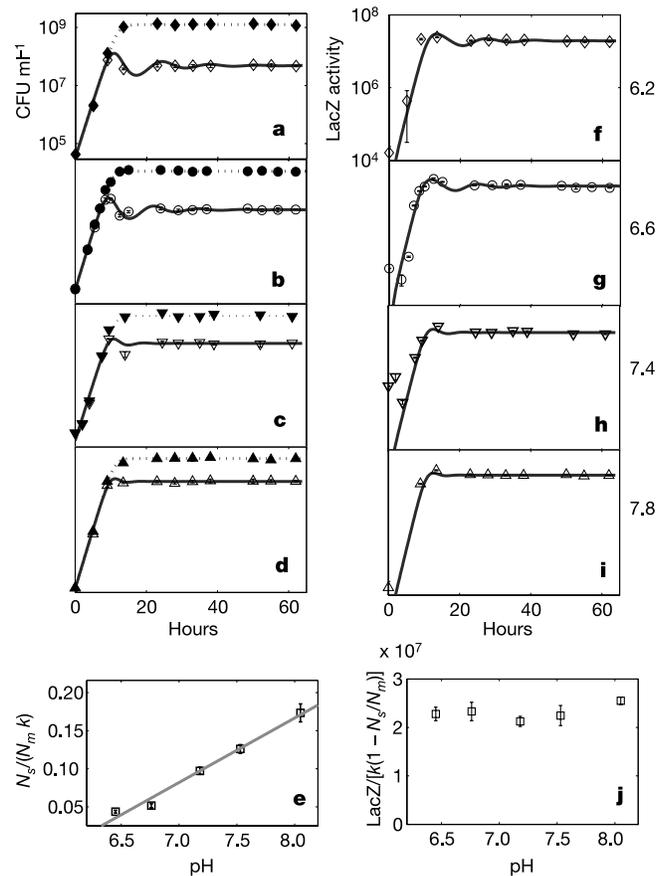

Figure 2 Experimentally measured growth curves (**a**) and corresponding levels of LacZα–CcdB (**b**) of Top10F′ cells with the population-control circuit OFF (filled squares) and ON (open squares) for pH 7.0. Model predictions are shown in solid (ON) and dotted (OFF) lines, except for the OFF case of LacZ activity, where the killer protein concentration is always zero in the model. The simulated LacZ activity is obtained by multiplying the simulated killer protein concentration (in nM) by a constant factor so that the experiment and simulation are at the same scale. Insets show the growth curves and the LacZ activity in linear scale for the ON case. The similar growth of two cultures at low cell density is an intrinsic feature of the circuit and is not caused by a lag in circuit activation. When the ON culture at steady state was diluted into fresh medium with and without the inducer, the resulting cultures again grew similarly at low density but deviated at high density.

Figure 3 Effects of pH on circuit behaviour. **a–d**, Cell growth with the circuit OFF (filled symbols) and ON (open symbols). **e**, Dependence of $N_s/(N_m \times k)$ on pH. **f–i**, Time courses of LacZ activity with the circuit ON. **j**, Dependence of $\frac{\text{LacZ activity}}{k(1-N_s/N_m)}$ on pH. Panels **a–d** have the same scale in both x and y axes, as do the panels (**f–i**). Simulated growth curves (ON, solid line; OFF, dotted line) and killer protein time courses (ON, solid line) are shown in **a–d** and **f–i**. The killer protein concentration for the OFF cases is always zero in the model. Simulated LacZ activity in **f–i** is obtained by multiplying the simulated killer protein concentration by a constant factor so that the experiment and simulation are at the same scale in each panel. In **e** and **j**, steady-state pH values (Table 1) are used along the x axes. In **e**, N_s is normalized with respect to N_m and k to account for minor variations in these variables (Table 1). The dependence of $N_s/(N_m \times k)$ on pH is nearly linear ($R^2 = 0.98$).

Table 1 Effects of pH on circuit parameters

Medium pH	Steady-state culture pH*	k†(h^{-1})	N_m per 10^9‡ (CFU ml^{-1})	N_s per 10^7§ (CFU ml^{-1})	d_A‖ (h^{-1})	LacZ activity/10^7¶ (fluorescence per (ml × OD 600))
6.2	6.45	0.885	1.25 ± 0.06	4.86 ± 0.02	0.274	1.94 ± 0.12
6.6	6.76	0.928	1.17 ± 0.05	5.59 ± 0.03	0.304	2.02 ± 0.17
7.0	7.18	0.970	1.24 ± 0.10	11.7 ± 0.6	0.639	1.87 ± 0.09
7.4	7.53	0.897	1.16 ± 0.10	13.1 ± 0.6	0.791	1.79 ± 0.16
7.8	8.05	0.936	1.20 ± 0.07	19.5 ± 1.3	1.19	2.00 ± 0.06

*Measured at about 50 h after growth initiation in ON cultures.
†Obtained by fitting the exponential phase of growth curves of OFF cultures.
‡Average of the stationary-phase cell density of OFF cultures between 28 h and 62 h.
§Average of the circuit-ON cell density between 28 h and 62 h.
‖Obtained by solving equation $N_s = \frac{N_m d_A d_E k}{N_m \nu_A k_E d + d_A d_E k}$ with d_A as the only unknown.
¶Average of LacZ activity of ON cultures between 28 h and 62 h.

Similar to multicellular organisms, bacteria possess sophisticated suicide machinery that is triggered by stress and starvation or by 'addiction modules' during post-segregational killing[16,23,24]. Natural systems, such as the signalling network that dictates the lysis of a subpopulation of *Streptococcus pneumoniae* at high cell density, employ a mechanism similar to our circuit of regulated killing coordinated by quorum sensing[23,25]. Owing to selection pressure, mutants that escape regulation by the synthetic population-control circuit usually arise 3 to 6 days after circuit activation (tested by dilution into fresh medium; data not shown). Although there are no direct measurements, escaping the regulation of natural systems is probably much rarer. The greater genetic stability of natural systems may be due to more sophisticated regulation or their coupling to other physiological processes, or both. For example, cell lysis is an essential stage of the development of natural transformation in *Streptococcus pneumoniae*, where survivors assimilate DNA released by lysed cells[25]. Thus, there may be a selection pressure favouring the overall signalling network (with the lysis-regulation network as a subset) responsible for this developmental process. Design concepts such as these can be tested by introducing additional regulatory modules into the population-control circuit or coupling the circuit to functions that are beneficial to the cells.

The population-control circuit lays the foundation for using cell–cell communication to programme interactions among bacterial communities, allowing the concept of communication-regulated growth and death to be extended to engineering synthetic ecosystems. The rich repertoire of natural quorum-sensing modules[13,14], supplemented by engineered counterparts[26,27], will facilitate construction of multichannel feedback systems where population densities are coupled to communications. □

Methods

Plasmids

Plasmid pLuxRI2 (ColE1 origin, chloramphenicol^R) was constructed by inserting polymerase chain reaction (PCR)-amplified *luxI* from pSND-1[28] into pLuxR2, downstream of *luxR*. pLuxR2 was made in two steps: (1) pLuxR encoding LuxR under the control of $p_{lac/ara-1}$ was constructed by inserting PCR-amplified *luxR* from pKE705[29] into pPROLar.A122 (BD Biosciences Clontech); (2) pLuxR2 was made by inserting a fragment containing $p_{lac/ara-1}$–*luxR* from restriction-digested pLuxR into pPROTet.E133 (BD Biosciences Clontech). Plasmid p*lux*CcdB3 (p15A origin, kanamycin^R) was constructed by PCR-fusing *lacZα–ccdB* from pZErO-2 (Invitrogen) to p_{luxI}, and inserting the fused DNA into pPROLar.A122. Plasmid p*lux*GFPuv contains p_{luxI} cloned from pKE555[15]. Both pLuxRI2 and p*lux*CcdB3 were confirmed by sequencing. Versions of the circuit constructed using different combinations of replication origins, promoters and CcdB variants with different lethality demonstrated similar phenotypes to those reported here.

Strains, growth conditions and media

Unless otherwise stated, Top10F′ cells (Invitrogen) were used throughout this study. Standard LB medium was used for cell growth to probe qualitative behaviour. For quantitative measurements, cells were grown in pH-buffered TBK medium (10 g tryptone and 7 g KCl per litre buffered with 100 mM weak acids). Medium pH (measured with Accumet pH Meter 925, Fischer Scientific) was adjusted by adding 5 M KOH. MOPS was used to buffer pHs between 7 and 8, and PIPES was used for pHs between 6.2 and 6.8. The buffered media were able to maintain pH well; variations in pH were <0.3 and mostly occurred within the first 24 h of growth. Plasmids were maintained with 100 μg ml^{-1} of

chloramphenicol and 50 μg ml^{-1} of kanamycin. One-millimolar IPTG was used to activate the circuit.

To measure circuit function, 3 ml LB in a 12 ml culture tube was inoculated from a single colony and incubated overnight at 30 °C and 250 r.p.m. When the culture reached an optical density (OD) between 0.1 and 0.3 (measured at 600 nm with a Spectra MAX250 microplate reader, Molecular Devices), the overnight culture was diluted 1,000-fold into 50 ml of fresh, buffered TBK in 250 ml flasks supplemented with antibiotics and IPTG when applicable. The flask cultures were incubated at 34 °C and 250 r.p.m. Antibiotics and the inducer were replenished about 50 h after inoculation with an additional 50 μg ml^{-1} of chloramphenicol, 25 μg ml^{-1} of kanamycin and 0.25 mM IPTG when applicable. Samples were drawn at different time points to measure the number of viable cells by serial dilution and plating (in triplicate), LacZ activity (see below) and OD.

LacZ assay

LacZα–CcdB levels were measured in triplicate using a FluoReporter LacZ/Galactosidase Quantitation kit (Molecular Probes). To permeate cells, 5 μl of chloroform was added to 200 μl of culture, which was vortexed vigorously for 30 s. Then 10 μl cell lysate was added to 100 μl of 1.1 mM 3-carboxyumbelliferyl-β-D-galactopyranoside (CUG) solution in each well of a 96-well microplate. The reaction mixture was incubated at room temperature for 30 min before fluorescence was measured (excitation, 390 nm; emission, 460 nm). Measured LacZ activity was corrected by subtracting the background fluorescence, measured in control wells containing 100 μl of CUG solution but no cell lysate. The corrected value was normalized to culture volume and OD 600 and expressed in fluorescence per (ml × OD 600). We observed that LacZα–CcdB caused cell death but did not destroy dead cells. Thus both live and dead cells contributed to LacZ activity. Normalizing the measured LacZ activity to total cell mass would thus give a good estimate of the intracellular killer protein concentration.

Mathematical modelling

We model the major kinetic events dictating the circuit function, including cell growth and death (equation (1)), and production and degradation of the killer protein (equation (2)) and the AHL signal (equation (3)). We assume that, (1) without the circuit, changes in viable cell density (N, ml^{-1}) follow logistic kinetics with an intrinsic per capita growth rate of k (h^{-1}) and a carrying capacity of N_m (ml^{-1}); (2) for circuit-regulated growth, the cell death rate is proportional to the intracellular concentration of the killer protein (E, nM) with a rate constant of d (nM^{-1} h^{-1}); (3) the production rate of E is proportional to AHL concentration (A, nM, assumed to be the same inside and outside the cells) with a rate constant of k_E (h^{-1}); (4) AHL production rate is proportional to N with a rate constant of ν_A (nM ml h^{-1}); and (5) degradation of the killer protein and AHL follows first-order kinetics with rate constants of d_E (h^{-1}) and d_A (h^{-1}).

$$\frac{dN}{dt} = kN(1 - N/N_m) - dEN \qquad (1)$$

$$\frac{dE}{dt} = k_E A - d_E E \qquad (2)$$

$$\frac{dA}{dt} = \nu_A N - d_A A \qquad (3)$$

In experiments, N and N_m are measured as colony-forming units per ml (CFU ml^{-1}). The production term ($k_E A$) in equation (2) lumps several intermediate steps together: activation of LuxR by AHL, binding of activated LuxR to p_{luxI}, and expression of the killer gene. It implies that the LuxR–AHL interaction is limited by the concentration of AHL, which is valid for our system (see main text). Although active LuxR functions as a dimer, we assume the cooperativity of AHL action to be 1, based on measurements for a closely related quorum-sensing system[30]. Assuming a greater cooperativity does not significantly affect model predictions. Equation (3) implies that the diffusion of AHL is fast compared with other processes and that the production rate of AHL from each viable cell is the same on average.

When $N \ll N_m$, equation (1) reduces to $\frac{dN}{dt} = (k - dE)N$. Then the simplified model will have two steady-state solutions: ($N_s = 0$, $E_s = 0$, $A_s = 0$) and (($N_s = \frac{d_A d_E k}{\nu_A k_E d}$, $E_s = k/d$, $A_s = \frac{d_E k}{k_E d}$), where subscript 's' represents steady state. Linear-stability analysis shows that the trivial steady state is unstable for all positive parameters, and the non-trivial steady state is stable if and only if $d_A + d_E > k$. Because the effective degradation rate constant of the killer protein inside the cell is at least its dilution rate constant caused by cell growth,

we have: $d_A + d_E > d_E > k$. Thus, the second steady state is stable for all biologically feasible parameters.

The analytical solution of the non-trivial steady state for the full model (equation (1)–equation (3)) can also be solved, in particular, $N_s = \frac{N_m d_A d_E k}{N_m v_A k_E d + d_A d_E k}$. This equation was used to deduce d_A (Table 1). In simulations (carried out using Dynetica[31]), the following parameters were kept at their base values: $d = 4 \times 10^{-3} \, \text{nM}^{-1} \, \text{h}^{-1}$, $k_E = 5 \, \text{h}^{-1}$, $d_E = 2 \, \text{h}^{-1}$, $v_A = 4.8 \times 10^{-7} \, \text{nM} \, \text{ml} \, \text{h}^{-1}$. The others ($k$, N_m and d_A) were computed from our experimental data (Table 1).

1. Becskei, A. & Serrano, L. Engineering stability in gene networks by autoregulation. *Nature* **405,** 590–593 (2000).

2. Gardner, T. S., Cantor, C. R. & Collins, J. J. Construction of a genetic toggle switch in *Escherichia coli*. *Nature* **403,** 339–342 (2000).

3. Atkinson, M. R., Savageau, M. A., Myers, J. T. & Ninfa, A. J. Development of genetic circuitry exhibiting toggle switch or oscillatory behavior in *Escherichia coli*. *Cell* **113,** 597–607 (2003).

4. Isaacs, F. J., Hasty, J., Cantor, C. R. & Collins, J. J. Prediction and measurement of an autoregulatory genetic module. *Proc. Natl Acad. Sci. USA* **100,** 7714–7719 (2003).

5. Elowitz, M. B. & Leibler, S. A synthetic oscillatory network of transcriptional regulators. *Nature* **403,** 335–338 (2000).

6. Yokobayashi, Y., Weiss, R. & Arnold, F. H. Directed evolution of a genetic circuit. *Proc. Natl Acad. Sci. USA* **99,** 16587–16591 (2002).

7. Weiss, R., Homsy, G. E. & Knight, T. Jr *Dimacs Workshop on Evolution as Computation* 275–295 (Springer, Princeton, 1999).

8. Farmer, W. R. & Liao, J. C. Improving lycopene production in *Escherichia coli* by engineering metabolic control. *Nature Biotechnol.* **18,** 533–537 (2000).

9. Chen, W., Kallio, P. T. & Bailey, J. E. Construction and characterization of a novel cross-regulation system for regulating cloned gene expression in *Escherichia coli*. *Gene* **130,** 15–22 (1993).

10. Ozbudak, E. M., Thattai, M., Kurtser, I., Grossman, A. D. & van Oudenaarden, A. Regulation of noise in the expression of a single gene. *Nature Genet.* **31,** 69–73 (2002).

11. Elowitz, M. B., Levine, A. J., Siggia, E. D. & Swain, P. S. Stochastic gene expression in a single cell. *Science* **297,** 1183–1186 (2002).

12. Blake, W. J., Kærn, M., Cantor, C. R. & Collins, J. J. Noise in eukaryotic gene expression. *Nature* **422,** 633–637 (2003).

13. Miller, M. B. & Bassler, B. L. Quorum sensing in bacteria. *Annu. Rev. Microbiol.* **55,** 165–199 (2001).

14. Fuqua, C., Parsek, M. R. & Greenberg, E. P. Regulation of gene expression by cell-to-cell communication: acyl-homoserine lactone quorum sensing. *Annu. Rev. Genet.* **35,** 439–468 (2001).

15. Egland, K. A. & Greenberg, E. P. Quorum sensing in *Vibrio fischeri*: elements of the *luxI* promoter. *Mol. Microbiol.* **31,** 1197–1204 (1999).

16. Engelberg-Kulka, H. & Glaser, G. Addiction modules and programmed cell death and antideath in bacterial cultures. *Annu. Rev. Microbiol.* **53,** 43–70 (1999).

17. Dong, Y. H. *et al.* Quenching quorum-sensing-dependent bacterial infection by an *N*-acyl homoserine lactonase. *Nature* **411,** 813–817 (2001).

18. Leadbetter, J. R. & Greenberg, E. P. Metabolism of acyl-homoserine lactone quorum-sensing signals by *Variovorax paradoxus*. *J. Bacteriol.* **182,** 6921–6926 (2000).

19. Schaefer, A. L., Hanzelka, B. L., Parsek, M. R. & Greenberg, E. P. Detection, purification, and structural elucidation of the acylhomoserine lactone inducer of *Vibrio fischeri* luminescence and other related molecules. *Methods Enzymol.* **305,** 288–301 (2000).

20. Hasty, J., McMillen, D. & Collins, J. J. Engineered gene circuits. *Nature* **420,** 224–230 (2002).

21. Weiss, R. *et al.* Genetic circuit building blocks for cellular computation, communications, and signal processing. *Nat. Comput.* **2,** 47–84 (2003).

22. Wall, M. E., Hlavacek, W. S. & Savageau, M. A. Design of gene circuits: lessons from bacteria. *Nature Rev. Genet.* **5,** 34–42 (2004).

23. Lewis, K. Programmed death in bacteria. *Microbiol. Mol. Biol. Rev.* **64,** 503–514 (2000).

24. Ameisen, J. C. On the origin, evolution, and nature of programmed cell death: a timeline of four billion years. *Cell Death Differ.* **9,** 367–393 (2002).

25. Steinmoen, H., Knutsen, E. & Havarstein, L. S. Induction of natural competence in *Streptococcus pneumoniae* triggers lysis and DNA release from a subfraction of the cell population. *Proc. Natl Acad. Sci. USA* **99,** 7681–7686 (2002).

26. Bulter, T. *et al.* Design of artificial cell–cell communication using gene and metabolic networks. *Proc. Natl Acad. Sci. USA* **101,** 2299–2304 (2004).

27. Gerchman, Y. & Weiss, R. Teaching bacteria a new language. *Proc. Natl Acad. Sci. USA* **101,** 2221–2222 (2004).

28. Weiss, R. & Knight, T. in *Sixth International Workshop on DNA-Based Computers, DNA 2000* (eds Codon, A. & Rozenberg, G.) 1–16 (Springer, New York, 2000).

29. Egland, K. A. & Greenberg, E. P. Quorum sensing in *Vibrio fischeri*: analysis of the LuxR DNA binding region by alanine-scanning mutagenesis. *J. Bacteriol.* **183,** 382–386 (2001).

30. Zhu, J. & Winans, S. C. Autoinducer binding by the quorum-sensing regulator TraR increases affinity for target promoters *in vitro* and decreases TraR turnover rates in whole cells. *Proc. Natl Acad. Sci. USA* **96,** 4832–4837 (1999).

31. You, L., Hoonlor, A. & Yin, J. Modeling biological systems using Dynetica—a simulator of dynamic networks. *Bioinformatics* **19,** 435–436 (2003).

32. Lutz, R. & Bujard, H. Independent and tight regulation of transcriptional units in *Escherichia coli* via the LacR/O, the TetR/O and AraC/I1-I2 regulatory elements. *Nucleic Acids Res.* **25,** 1203–1210 (1997).

Correspondence and requests for materials should be addressed to F.H.A (frances@cheme.caltech.edu).